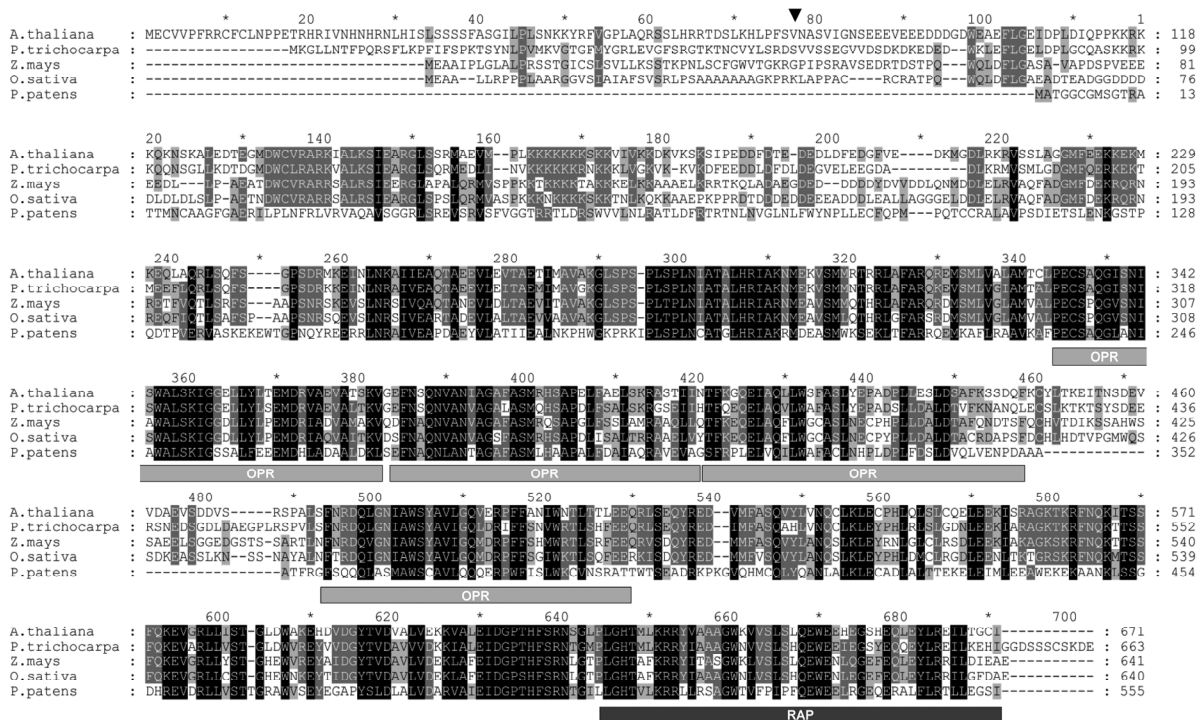


**A**



**B**

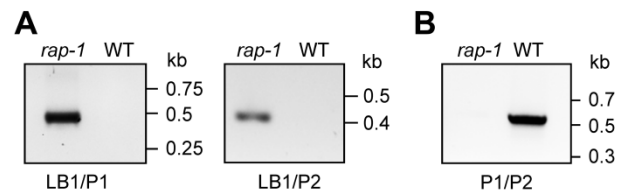
	TargetP <sup>1</sup>	Predotar <sup>2</sup>	WoLF PSORT <sup>3</sup>
<i>A. thaliana</i>	C	(C)	(C)
<i>P. trichocarpa</i>	M	(M)	C
<i>Z. mays</i>	C	C	C
<i>O. sativa</i>	C	-	C
<i>P. patens</i>	C	(C)	C

<sup>1</sup>Emanuelsson et al. 2000, <sup>2</sup>Nielsen et al. 1997, <sup>3</sup>Small et al. 2004; <sup>3</sup>Paul et al. 2007

**Supplemental Figure 1.** Sequence Alignment and Targeting Predictions for RAP and its Orthologs in Higher Plants and Moss.

**(A)** Multiple sequence alignment of RAP (*A. thaliana*) and orthologous proteins from *P. patens* (*Physcomitrella patens*), *P. trichocarpa* (*Populus trichocarpa*), *Z. mays* (*Zea mays*) and *O. sativa* (*Oryza sativa* cv. *Japonica*). Sequence accession numbers are in Methods. The alignment was generated using ClustalW (Thompson et al. 2002) and displayed with Genedoc (<http://www.psc.edu/biomed/genedoc>; Nicholas et al. 1997). Shading as in Figure 8. OPR repeats and the RAP domain (pfam08373) are indicated. The cleavage site in the chloroplast transit peptide predicted by TargetP (Nielsen et al. 1997; Emanuelsson et al. 2000) is designated for RAP by the filled triangle above the sequence.

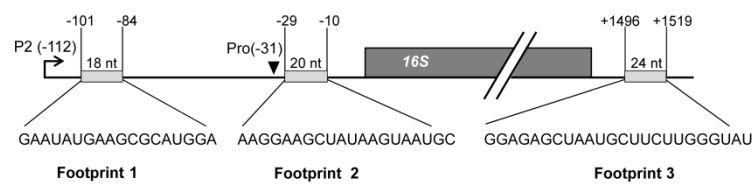
**(B)** Targeting predictions for proteins shown in (A). C: chloroplast, M: mitochondria. Parentheses indicate a possible localization in the respective organelle.



**Supplemental Figure 2. PCR Analysis of *rap-1* Mutants.**

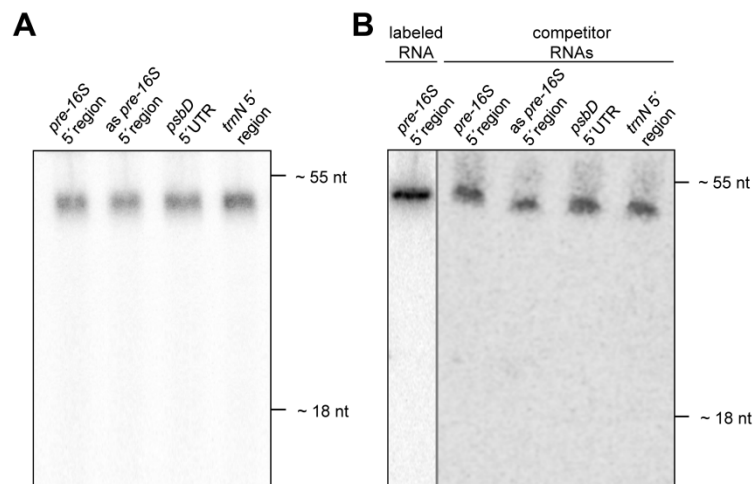
**(A)** Determination of T-DNA insertion site in *rap-1*. PCR analysis was performed with primers LB1/P1 (left panel) and LB1/P2 (right panel) which amplify a sequence from both sites of the T-DNA insertion allele in *RAP* and the genomic flanking sequence. PCR products obtained were separated on an agarose gel alongside a size marker (marker lane not displayed) and subjected to sequence analysis to determine the exact site of T-DNA insertion. The positions of the gene- and T-DNA-specific primers used are depicted in Figure 2A.

**(B)** Identification of mutants homozygous for the insertion in *RAP*. PCR analysis was performed with primers P1 and P2 which bind to the *RAP* gene up- and downstream of the T-DNA insertion site in *rap-1*. PCR products were separated on an agarose gel alongside a size marker (marker lane not displayed). For positions of primers see Figure 2A.



**Supplemental Figure 3.** Distribution of Footprints within the 16S rRNA Precursor.

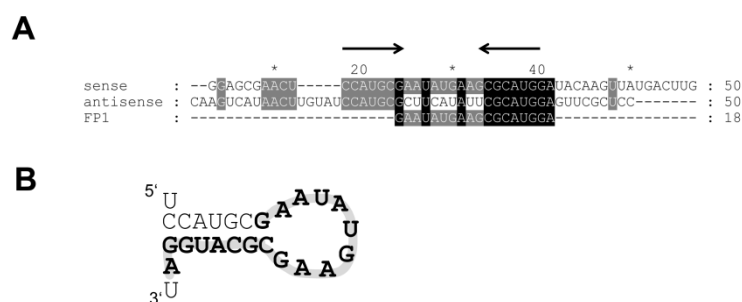
Positions of the PEP promoter (P2, -112) and the precursor processing site (Pro, -31) are indicated with respect to the 5' end of the mature transcript. Footprints identified by Ruwe and Schmitz-Linneweber (2012) are depicted as light grey boxes with given length and nucleotide sequences.



**Supplemental Figure 4. Integrity of Probes used for RNA Binding Assays in Figure 6.**

**(A)** Integrity of probes used for binding curves (Figure 6A). 3 fmol of labeled RNA were loaded on a denaturing 10% polyacrylamide gel. The dye migration of xylene cyanol (~55 nt) and bromophenol blue (~18 nt) is indicated on the right. Slight differences in signal intensities of the competitor RNAs correlate with numbers of radiolabeled U-residues in each transcript.

**(B)** Integrity of probes used for competition experiments (Figure 6B). 3 fmol of labeled RNA or 30 fmol of respective competitor RNAs (labeled with 1/1000 of  $^{32}\text{P}$  UTP) were loaded on the same denaturing 10% polyacrylamide gel. As indicated by a grey line, the left part of the gel showing the competitor RNAs was exposed ten times longer than the right part and the contrast was adjusted to visualize the signals. The dye migration of xylene cyanol (~55 nt) and bromophenol blue (~18 nt) is indicated on the right. Slight differences in signal intensities of the competitor RNAs correlate with numbers of radiolabeled U-residues in each transcript.



**Supplemental Figure 5. Formation of a Potential Stem Loop Structure at the 16S rRNA Precursor 5' End.**

**(A)** Sequence alignment of the 16S precursor sense and antisense probes and the putative RAP binding site (FP1) displayed with Genedoc (Nicholas et al. 1997). The two inverted sequences which have the potential to form the stem loop structure shown in **(B)** are indicated by arrows above the sequences.

**(B)** Potential stem loop structure formed overlapping the RAP binding site. The binding site (FP1) is highlighted in grey and written in bold letters.

## Supplemental References

- Emanuelsson, O., Nielsen, H., Brunak, S. and von Heijne, G.** (2000). Predicting subcellular localization of proteins based on their N-terminal amino acid sequence. *J. Mol. Biol.* **300**: 1005-1016.
- Nicholas, K. B., Nicholas, H. B. and Deerfield, D. W.** (1997). GeneDoc: analysis and visualization of genetic variation. *EMBNET. NEWS* **4**: 14.
- Nielsen, H., Engelbrecht, J., Brunak, S. and von Heijne, G.** (1997). Identification of prokaryotic and eukaryotic signal peptides and prediction of their cleavage sites. *Protein Eng.* **10**: 1-6.
- Ruwe, H. and Schmitz-Linneweber, C.** (2012). Short non-coding RNA fragments accumulating in chloroplasts: footprints of RNA binding proteins? *Nucleic Acids Res.* **40**: 3106-3116.
- Thompson, J. D., Gibson, T. J. and Higgins, D. G.** (2002). Multiple Sequence Alignment Using ClustalW and ClustalX. *Current Protocols in Bioinformatics*, John Wiley & Sons, Inc.